

FM Mode-Locking Fiber Laser

Inmar N. Ghazi*  Waleed Y. Hussein* & Salam Sami M. Salih*

Received on:1/4/2008

Accepted on: 26/6/2008

Abstract:

In this paper the study of Frequency Modulation Harmonic Mode-locking for Ytterbium Doped Fiber Laser is presented. The model studied, uses ytterbium-doped, single mode fiber pumped by 976 nm laser source is used with 150 mW pumping power to produce 1055 nm output laser and Frequency Modulation Harmonically Mode-Locked by MZI optical modulator. The effect of both normal and anomalous dispersion regimes on output pulses is investigated. Also, modulation frequency effect on pulse parameters is investigated by driving the modulator into different frequencies values.

This study shows the stability of working in anomalous dispersion regime and the pulse compression effect is better than counterpart normal regime, due to the combination effect

of both negative(Group velocity dispersion), GVD and nonlinearity. Also it shows the great effect of modulation frequency on pulse parameters and stability of the system. Model-locking fiber laser master equation is introduced, and using the assumed pulse shapes for both dispersion regimes after modifying (Ginzburg-Landau equation), GLE and by applying the moment method, a set of five ordinary differential equations are introduced describing pulse parameters evolution during each roundtrip. To solve these equations numerically using fourth- fifth order, Runge-Kutta method is performed through MatLab 7.0 program.

Key words:

Fiber Laser, Ytterbium Doped Fiber, Dispersion, FM Mode Locking, Pulse Propagation, Moment Method, Mat-Lab Program Design, Pulse Chirp, Pulse Energy, Pulse Width.

(1055mW) (150mW) (976nm)
(Mach-Zender Interferometer)
()
GVD
Ginzburg-Landau)
(equation
- -
.MatLab 7.0 (Runge-Kutta)

Nomenclature

$A(t,z)$	Slowly Varying Envelope of the Electric Field	
a	Pulse Amplitude	
c	Light Velocity	m/s
L	Cavity Length	m
E_{\max}	Peak Pulse Energy	pJ
F_m	Modulation Frequency	GHz
F_r	Repetition or Modulation Frequency	GHz
\bar{g}	Saturation	m^{-1}
\bar{g}_0	Average small-signal gain	m^{-1}
$M(A, t)$	Mode-Locker Term	
N	Number of Light Modes	
P_{ave}	Average power	mW
P_{sat}	Saturation Power	mW
q	Chirp Factor	
RT	Roundtrip	
T	Propagation Time	μs
T_R	Roundtrip Time	μs

Greek Letters

$\bar{\alpha}$	Average Losses	m^{-1}
----------------	----------------	----------

$\overline{\beta}_2$	Averaged Second Order Dispersion	fs^2 / m
$\overline{\beta}_3$	Averaged Third Order Dispersion	fs^3 / m
$\overline{\gamma}$	Average Non Linearity	$(\text{mW})^{-1}$
ΔE	Variation between Maximum and Minimum Energy Value	pJ
Δ_{FM}	Modulation Depth	
Δ_{ω}	Gain Medium Spectral Full Width at Half-Maximum	rad/fs
ξ	Temporal Shift	ps
μm	Micro-Meter	
τ	Pulse Width	ps
φ	Phase Shift	rad
Ω	Frequency Shift	GHz
ω_m	Modulation Frequency = $2\pi(F_r)$	

1. Introduction:

Mode-locked lasers are routinely used for a wide variety of applications since they can provide optical pulses ranging in widths from a few femtoseconds to hundreds of picoseconds. As early as 1970, an analytic theory was developed for determining pulse parameters and shape in actively mode-locked solid-state lasers by considering the effects of the mode-locker and gain filtering and then imposing a self-consistency criterion in the time domain. In many cases, it is possible to include the effect of chromatic dispersion on the pulse shape as well; however, once the nonlinear effects within the cavity become important, analytic investigations begin to falter.

closed form solution, passive mode-locking mechanisms, such as nonlinear polarization rotation, nonlinear fiber-loop mirror, and saturable absorption, produce “soliton-like” pulses.

The purpose is to obtain the basic equation that satisfies propagation of optical pulses in single-mode fibers. Then the equations that concern the evolution of pulse parameters during each roundtrip will be introduced.

These equations will be solved numerically using fourth-fifth order Runge-Kutta.

2. Mode-Locking Fiber Laser Master Equation:

A general “master” equation used to model mode-locking fiber laser system is introduced.

This equation, is in fact a Generalized Non-Linear Schrödinger Equation (GNLSE) or (Ginzburg-Landau equation) [5, 6] which, generally describes all types of mode-locking fiber lasers by just changing the term $M(A, t)$ that represents the mode-locker technique. The mode-Lock master equation is: [1, 7, 8]

$$T_R \frac{\partial A}{\partial T} + \frac{i}{2} (\bar{\beta}_2 + i\bar{g}T_2^2) L \frac{\partial^2 A}{\partial t^2} - \frac{\bar{\beta}_3}{6} L \frac{\partial^3 A}{\partial t^3} = \bar{\gamma} L |A|^2 A + \frac{1}{2} (\bar{g} - \bar{\alpha}) LA + M(A, t) \dots \dots \dots (1)$$

Where, the saturation gain \bar{g} , could be approximated as in following relation:

[7, 6, 8]

$$\bar{g} = \bar{g}_0 / (1 + P_{ave} / P_{sat}) \dots \dots \dots (2)$$

Where, P_{sat} represents the saturation power of the gain medium, \bar{g}_0 the average small-signal gain, and, P_{ave} the average power over one pulse slot of duration T_m , which be calculated as in the following equation: [9, 10]

$$P_{ave} = \frac{1}{T_m} \int_{-\frac{T_m}{2}}^{+\frac{T_m}{2}} |A(t, z)|^2 dt \dots \dots \dots (3)$$

The term $A(t, z)$, represents the slowly varying envelope of the electric field and the pulse slot is calculated by following equation:

$$T_m = 1/F_r = T_R / N \dots \dots \dots (4)$$

Where F_r is the frequency at which the laser is mode-locked, which is often denoted

F_m as modulation frequency. N is an integer ($N \geq 1$) representing the harmonic at which the laser will mode locked. T_R , is the roundtrip.

The gain medium's finite bandwidth is assumed to have a parabolic filtering effect with a spectral full width at half-maximum (FWHM) which is given by following relation: [5]

$$\Delta_\omega = 2/T_2 \dots \dots \dots (5)$$

Where:

T_2 : The spectral width of the finite gain bandwidth.

The term $i\bar{g}T_2^2$, results from the gain. The physical origin of this contribution is related to the finite gain band width of the doping fiber and is referred to as gain dispersion ($\bar{g}T_2^2$) since it originates from the frequency dependence of the gain. [5]

The term (A) is the slowly varying envelope of the electric field in term of T , the propagation time, which is given by the following relation:

$$T = z/v_g \dots \dots \dots (6)$$

Where:

z : the propagation distance in z direction,

v_g : the group velocity.

In the master equation, Eq. (1), there are two time scales which represent:

1. The time (t), measured in the frame of the moving pulse.

2. The propagation time (T).

Since an average over a single roundtrip is considered, (T) is measured in terms of the roundtrip time:

$$T_R = L / v_g = c / 2nL \dots\dots\dots (7)$$

Where:

L : The cavity length

n : Refractive Index

The pulse time scale is assumed to be sufficiently smaller than T_R and hence, the two times are essentially decoupled. [11]

This treatment is valid for most mode-locked lasers for which T_R exceeds 1 ns and pulse widths are typically less than ps.

The effect of FM mode-locker on the field is sinusoidal and as in the following expression: [12, 7]

$$M(A, t) = i\Delta_{FM} \cos \omega_m (t + t_m) A \dots (8)$$

Where:

Δ_{FM} : Modulation depth,

t_m : The delay between the center of the modulation cycle and the temporal window in which the pulses are viewed, and

ω_m : Modulation frequency (assumed to be identical to that of the mode-locked pulse train in this work), i.e.

$$\omega_m = 2\pi(F_r) \dots\dots\dots (9)$$

The over bar in Eq. (1) refer to the averaged value of the corresponding parameter. For example, $\bar{\beta}_2, \bar{\beta}_3, \bar{\alpha}$ and $\bar{\gamma}$ represent the second-order dispersion, third order dispersion (TOD), loss, and nonlinearity, respectively, are averaged over the cavity length.

3. Moment Method:

As shown in previous section, mode-locked fiber lasers are governed by nonlinear partial differential equation Eq. (1), which generally, does not posses analytic solution [10] and, hence to model the pulse that produces. Another drawback, it gives the final pulse shape, it does not explain how does the pulse evolutes during each roundtrip.

To solve it numerically by one of numerical solution method such as split or wavelet method [3], all parameters need to be considered including TOD and mode-locker effect. The last two parameters have great effect on pulse shape and stability.

As a result, to solve such third order partial deferential equation, initial conditions and boundary conditions need to be known. Moreover, longtime required for computer program to implement such numerical solution.

It is useful to convert this third order partial differential equation to a set of ordinary differential equations which describe the evolution of pulse parameters during each roundtrip. [7] These pulse parameters evolution equations are obtained using so-called moment method. [10, 13]

Using moment method pulse parameters equations, it is possible to study the pulse evolution process under the effect of Eq. (1), with no need to full numerical simulation.

4. Pulse Parameters Evolution Equation:

Depending on master equation Eq. (1) and using the assumed pulse shapes for both dispersion regimes after modifying Ginzburg-Landau Equation, GLE, by adding TOD and mode-locker effects, the extended solution will be as in the following relations: [7, 9, 10, 13].

a. Normal regime:

$$A(T, t) = a \left(\exp \left(- \frac{(t - \xi)^2}{2\tau^2} \right) \right)^{1+iq} \times \exp(i\Omega(t - \xi) + ikT + i\phi_0) \dots\dots\dots (10)$$

b. Anomalous regime:

$$A(T, t) = a \left(\operatorname{sech} \left(\frac{t - \xi}{\tau} \right) \right)^{1+iq} \times \exp(i\Omega(t - \xi) + ikT + i\phi_0) \dots\dots\dots (11)$$

Where pulse parameters for both profiles are:

(a) : pulse amplitude,

(ξ) : Temporal shift,

(τ) : pulse width,

(q) : chirp,

(Ω) : frequency shift,

$ikT + i\phi_0$: represents the phase and rarely is of physical interest in lasers producing picoseconds pulses, which will be ignored. [14]

A set of five equations are introduced (Appendix A) describing pulse parameters evolution during each roundtrip: [7, 10, 14]

$$\frac{T_R}{L} \frac{dE}{dT} = (\bar{g} - \bar{\alpha})E \times \frac{\bar{g}T_2^2}{2\tau^2} (C_0(1+q^2) + 2\Omega^2\tau^2)E \dots (12)$$

$$\frac{T_R}{L} \frac{d\xi}{dT} = \bar{\beta}_2\Omega - \bar{g}T_2^2q\Omega + \frac{\bar{\beta}_3}{4\tau^2} (C_0(1+q^2) + 2\Omega^2\tau^2) \dots (13)$$

$$\frac{T_R}{L} \frac{d\Omega}{dT} = -C_0 \frac{\bar{g}T_2^2}{\tau^2} (1+q^2)\Omega + \frac{\Delta_{FM}\omega_m}{L} \psi_0 \times \sin(\omega_m(\xi - t)) \dots (14)$$

$$\frac{T_R}{L} \frac{dq}{dT} = \frac{\bar{\beta}_3}{\tau^2} (C_0(1+q^2) + 2\Omega^2\tau^2) - \frac{\bar{g}T_2^2}{\tau^2} q(C_0(1+q^2) + 2\Omega^2\tau^2) + C_2 \frac{\bar{\gamma}E}{\sqrt{2\pi\tau}} + \frac{\bar{\beta}_3\Omega}{\tau^2} \left[\frac{3}{2C_0} (1+q^2) + \Omega^2\tau^2 \right] + \frac{\Delta_{FM}\omega_m\tau}{L} \psi_1 \cos(\omega_m(\xi - t)) \dots (15)$$

$$\frac{T_R}{L} \frac{d\tau}{dT} = C_3 \frac{\bar{\beta}_2}{\tau} q + C_3 \frac{\bar{\beta}_3}{\tau} q\Omega + C_0C_3 \frac{\bar{g}T_2^2}{2\tau} (C_4 - q^2) \dots (16)$$

Where the constants C_n ($n=0$ to 4) are introduced.

In case of Gaussian pulse:

$$1. C_0 = C_1 = C_2 = C_3 = C_4 = 1$$

$$2. \psi_0 = \exp\left(-\frac{\omega_m^2\tau^2}{4}\right) \dots (17)$$

$$3. \psi_1 = \omega_m\tau\psi_0 \dots (18)$$

In the case of an auto solution,

$$1. C_0 = 2/3,$$

$$2. C_1 = 1/3,$$

$$3. C_2 = \sqrt{2\pi}/3,$$

$$4. C_3 = 6/\pi^2,$$

$$5. C_4 = 2.$$

$$6. \psi_0 = \left(\frac{\pi\omega_m\tau}{2}\right) \csc h\left(\frac{\pi\omega_m\tau}{2}\right) \dots (19)$$

$$7. \psi_1 = \left(\pi \coth\left(\frac{\pi\omega_m\tau}{2}\right) - 2/(\omega_m\tau)\right) \psi_0 \dots (20)$$

Since the accuracy of this approach depends upon the knowledge of exact pulse shape, it needs for master equation Eq. (1) to be solved numerically for more accuracy. A numerical solution for these five equations, using the fourth order Runge-Kutta method demonstrates that steady-state values obtained are deviate from the values obtained by direct solution of Eq. (1) by: (less than 3%) in the anomalous dispersion regime and (less than 12%) in the normal dispersion regime. [7, 10]

Hence, these results justify the use of the moment method and the pulse shapes assumed.

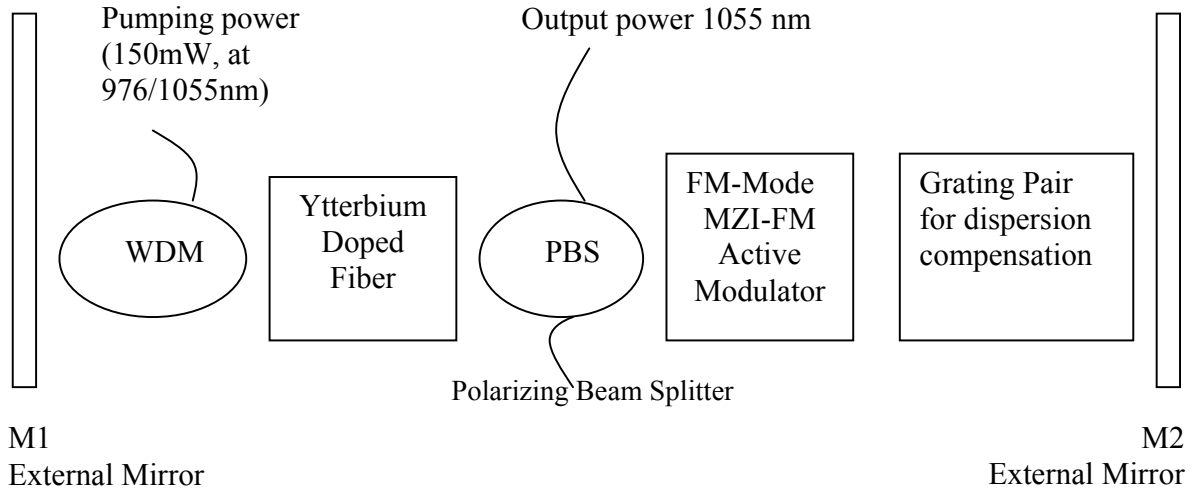


Fig (1) Block diagram model

Since the work is below zero dispersion wavelength ($1.22 \mu\text{m}$), (the used laser wavelength is $1.055 \mu\text{m}$) where normal dispersion GVD must compensated, a grating pair usually used to derive the system into anomalous regime. [15, 16] This will make the balancing between negative GVD and nonlinearity leading to pulse compression [17]. See Fig. (1) describing the simulation.

Where:

WDM: Wavelength Division Multiplexing

PBS: Polarizing Beam Splitter.

5. Results And Discussions:

Five equations are introduced using moment method which describes pulse parameters evolution at each round trip. To solve these equations numerically, a Mat-lab program has been written using fourth-fifth order Runge-Kutta method which uses the function ODE-45. This method is used to solve ordinary differential equations numerically. Ytterbium doped fiber pumped by 976 nm laser source is used with 150mW pumping power to produce 1055 nm output laser. [9] Mat-Lab 7.0 program uses the constants in Table (1), with the following initial values for pulse parameters: [7]

$$E(0) = 1 \text{ fJ}, \quad \xi(0) = 0, \quad \Omega(0) = 0, \quad q(0) = 0, \quad \tau(0) = 0.5 \text{ ps}.$$

A numerical solution will be done for both normal and anomalous dispersion regime. In normal dispersion regime, GVD has positive values i.e. $\bar{\beta}_2 > 0$ and solution will be done for both cases of TOD: $\bar{\beta}_3 = 0$ and $\bar{\beta}_3 = 30 \times 10^4 \text{ fs}^3/\text{m}$, to study TOD effect on pulse parameters. Executing the computer program, results of pulse parameters evolution plotted in Fig. (2) and Fig. (3). Fig. (2) (a and b), for pulse energy evolution plots, shows that there is no difference in behavior for both cases of TOD ($\bar{\beta}_3 = 0, \bar{\beta}_3 \neq 0$). Also, E reaches its maximum value $E_{\text{max}} \approx 2.795 \text{ pJ}$ in about 125 roundtrips while in anomalous regime where $\bar{\beta}_2 < 0$ the same E_{max} is achieved too, but in 75 round trips, (as shown in Fig (4) (a). Then damping oscillation occurs over thousands of roundtrips where $\Delta E = 0.015 \text{ pJ}$ (ΔE represents variation between maximum and minimum value)

decreasing in magnitude until steady state is achieved. The presence of third order dispersion (TOD) has big effect on pulse shape especially for ultra-short pulses of width in range ($\tau < 1$ p s), so it is

necessary to include the β_3 parameter, since it distorts the pulse by broadening it asymmetrically, thus producing a temporal and frequency shift.

As shown in Fig. (2) (a and b), in the absence of TOD, no temporal shift ($\xi = 0$), while in the presence of TOD, at temporal shift is introduced with positive and negative oscillation, not symmetrical around zero axis, $\Delta\xi \approx 90$ fs (variation between maximum and minimum) finally it converges to zero.

The same effect for TOD on pulse frequency shift, when $\beta_3 = 0$, no frequency

shift is introduced and thus $\Omega = 0$, while if β_3 has a value, a negative frequency shift is introduced with negative oscillation, then decreasing with increasing roundtrips, converges to zero steady state. As shown in Fig. (2) for frequency shift plot, most frequency shift is negative however, $\Delta\Omega \approx 21.5$ GHz and $\Omega \approx 2$ GHz at $RT = 4000$. While to achieve zero frequency shift, $RT_{ss} \gg 4000$. In Fig. (4a), pulse frequency shift evolution during first roundtrips is shown.

As shown in Fig. (3) (a) and (b), no effect for TOD on pulse chirp. In fact normal dispersion produces positive pulse chirp, oscillating around zero chirp axis until reaches zero, its steady-state value. Oscillation is symmetrical around zero chirp axes with $\Delta q \approx 16$, decreases as roundtrips increase, again $RT_{ss} \gg 4000$. From plots of pulse width evolution as in Fig. (3) (a) and (b), for pulse width plots, a broadening in pulse width is introduced with maximum width ($\tau_{max} = 8$ ps) in first 125 roundtrips,

then exhibits damped oscillation ($\Delta\tau \approx 7$ ps) over thousands of roundtrips decreasing to steady-state value ($\tau_{ss} \approx 3$ ps), where large number of roundtrips is needed $RT_{ss} \gg 4000$. From the plot of pulse chirp versus pulse width as in Fig. (3), it is clear that state is far to achieve unless large number of roundtrips has to be introduced. In Fig. (4b), pulse chirp and width evolution are shown during first roundtrips.

6. Effect Of Changing Modulation Frequency Of Pulse Parameters:

Since our model considers FM-Mode-locking fiber laser type, we will study the effect of changing modulation frequency on pulse parameters evolution using the same privies (table 1) but for different values of Fr (Fr=2.5-30GHz).

In both dispersion regimes the effect of changing modulation frequency, on pulse parameters is as shown in Fig. (5) & Fig. (6).

7. Conclusion And Future Work:

In the present study and its numerical results could be concluded regarding comparison between both dispersion regimes, and modulation frequency effect as follow:

- For variable frequency modulation, it is obvious that it affected on all pulse parameters in addition to the system stability without exception.
- Modulation frequency affect strongly on pulse parameters evolution. This can be seen from big oscillation parameter values during roundtrips for certain values of F_r ($F_r = 5$ GHz).
- Modulation frequency does not affect on parameter sign value,

Table (1) Constant for numerical solution [7]

parameter	value	parameter	value
$\bar{\beta}_2$	$\pm 1.4 \times 10^4 \text{ fs}^2 / \text{m}$	$\bar{\beta}_3$	$30 \times 10^4 \text{ fs}^3 / \text{m}$
$\bar{\gamma}$	$0.012(\text{mW})^{-1}$	$\bar{\alpha}$	0.17m^{-1}
\bar{g}_0	0.55m^{-1}	T_2	47 f s/rad
P_{sat}	25 mW	L	4 m
T_R	40 ns	F_r	10 GHz
Δ_{FM}	0.45	t_m	0
λ	1055 nm		

since they depend mainly on dispersion regime.

- Comparing plots of pulse parameter as function of F_r for both dispersion regimes of pulse energy and temporal shift, it is clear that they are almost equal with same behavior except in the number of roundtrips required for peak and steady-state values which is in anomalous less than in normal as stated earlier.
- Steady-state situation achievement possibility increases as F_r increases. This is clear in normal regime from plots of pulse chirp versus pulse width. While for anomalous there is a slight deviation from steady-state situation as F_r increases. However, F_r plays significant role in system stability.
- The frequency shift and chirp pulse plots for both regimes show

that the normal regime affected by F_r changes much more than in anomalous regime, and unaffected for high F_r values, i.e. $F_r > 5 \text{ GHz}$.

References

- [1.] G. P. Agrawal, "Nonlinear Fiber optic" (Academic Press, New York, 1995), second edition.
- [2.] G. Keiser, "Optical Fiber Communications", McGraw-Hill, Inc., New York, 2nd edition, (1991).
- [3.] Lionel R. Watkins, and Yu Rong Zhou, "Modeling propagation in optical Fibers Using Wavelets", Journal of Light wave Technology, Vol. 12, No.9, Sep. (1994).
- [4.] Andrew T. Ryan and Govind P. Agrawal, "Pulse compression and spatial phase modulation in normally dispersive nonlinear Kerr media", Optics Letts., Vol. 20, No. 3 Feb. (1995).
- [5.] M. Hofer, M. H. Ober, F. Haberl, and M. E. Fermann, "Characterization of Ultra-short pulse Formation in passively Mode-locked Fiber Lasers", IEEE Journal of Quantum Electronics. Vol. 28, No. 3. Mar. (1992).

- [6.] L. W. Liou and Govind P. Agrawal, "effect of frequency chirp on solution spectral sidebands in fiber laser" Optics Letts, Vol. 20, No. 11, Jun.,(1995).
- [7.] N. G. Usechak and G.P. Agrawal, "Rate-equation approach for frequency modulation mode locking using the moment method," J. Opt. Soc. Am. B, Vol. 22, pp 2570-2580(2005).
- [8.] Hermann A. Haus, and Yaron Silberberg, "Laser Mode Locking with Addition of Nonlinear Index", IEEE Journal of Quantum Electronics, Vol. QE-22, No. 2, Feb. (1986).
- [9.] Nicholas G. Usechak, Govind P. Agrawal, and Jonathan D. Zuegel, "FM Mode- Locked Fiber Lasers Operating in the Autosoliton Regime", IEEE Journal of Quantum Electronics, Vol. 41, No. 6, Jun. (2005).
- [10.] Jayanthi Santhanam and Govind P. Agrawal, "Raman-Induced Timing Jitter in Dispersion-Managed, Optical Communication Systems", IEEE Journal of Selected Topics in Quantum Electronics, Vol. 8, No. 3, May/ Jun. (2002).
- [11.] Guido H. M. van Tartwijk and Govind P. Agrawal, "Maxwell-Bloch dynamics And Modulation instabilities in fiber laser and amplifiers" J. Opt. Soc. Am. B, Vol. 14, No. 10, Oct. (1997).
- [12.] Herman A. Haus, "Mode-Locking of Lasers", IEEE Journal on Selected Topics in Quantum Electronics, Vol. 6, No. 6, Nov./Dec.(2000).
- [13.] Johan B. Geddes, Willie J. Firth and Kelly Black, "Pulse Dynamics in an Actively Mode-Locked Laser", Siam Journal applied Dynamical Systems, Society for Industrial and Applied Mathematics Vol. 2, No. 4, pp. 671,(2003).
- [14.] N. G. Usechack and G. P. Agrawal, "Semi-analytic technique for analyzing mode- locked lasers," Opt. Express , Vol. 13, pp 2075-2081 (2005).
- [15.] O. G. Okhotnikov, L. A. Gomes, N. Xiang, T. Jouhti, A. K. Chin, R. Singh, and A. B. Grudinin, "980-nm Pico-second Fiber Laser" IEEE Photonics Technology Letts, Vol. 15, No. 11, Nov. (2003).
- [16.] D. Foursa, P. Emplit, R. Leners and L. Meuleman, "18GHz from a o-cavity Er-fiber laser with dispersion management and rational harmonic active mode-locking" Electronics Letts , Vol.33 No. 6, March(1997).
- [17.] R.M. Mu, V.S. Grigoryan, Curtis R. Menyuk, G. M. Carter, and J. M. Jacob, "Comparison of Theory and Experiment for Dispersion-Managed Solutions in a Recirculating Fiber Loop", IEEE Journal of Selected Topics in Quantum Electronics, Vol. 6, No. 2, Mar./Apr. (2000).

Appendix A

The relation of pulse parameters with the temporal pulse profile are as following: [7, 10, 13]

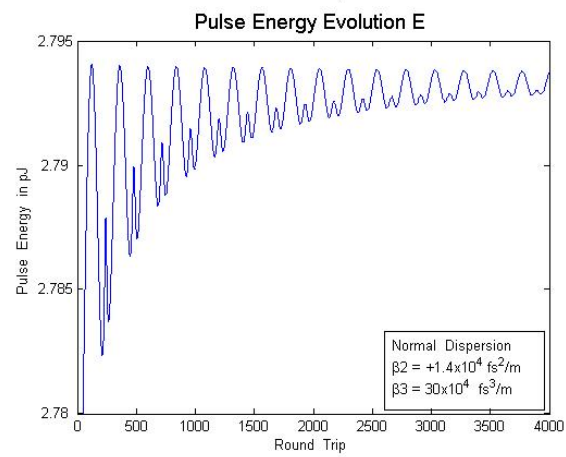
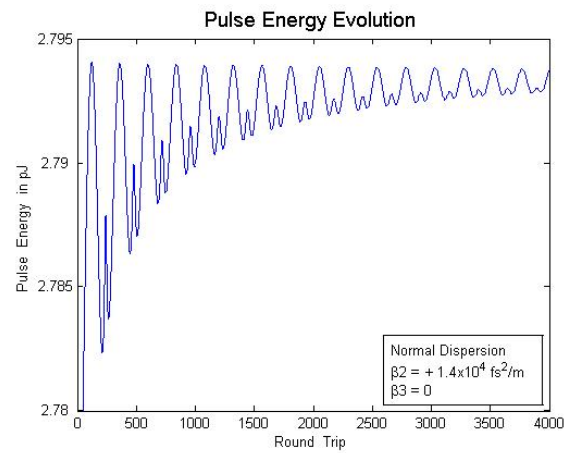
$$E(T) = \int_{-\infty}^{\infty} |A(T, t)|^2 dt \dots\dots\dots (A.1)$$

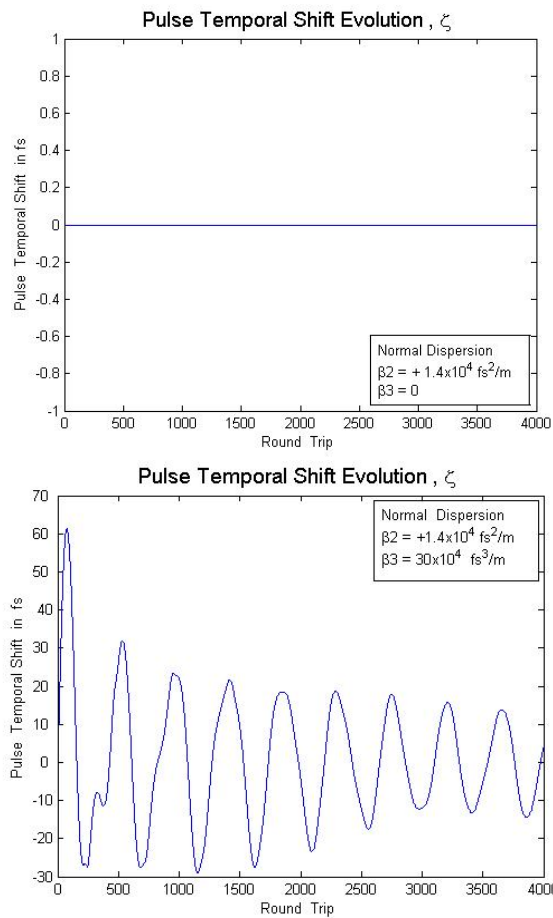
$$\xi(T) = \frac{1}{E} \int_{-\infty}^{\infty} t |A(T, t)|^2 dt \dots\dots\dots (A.2)$$

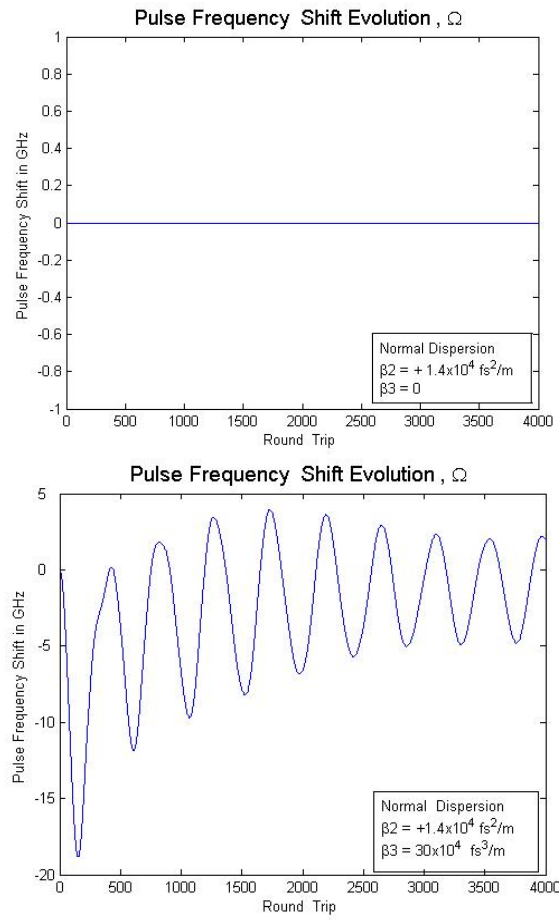
$$\Omega(T) = \frac{i}{2E} \int_{-\infty}^{\infty} [A^* \frac{\partial A}{\partial t} - A \frac{\partial A^*}{\partial t}] dt \dots\dots\dots (A.3)$$

$$q(T) = \frac{i}{E} \int_{-\infty}^{\infty} (t - \xi) [A^* \frac{\partial A}{\partial t} - A \frac{\partial A^*}{\partial t}] dt \dots\dots\dots (A.4)$$

$$\tau^2(T) = \frac{2c_3}{E} \int_{-\infty}^{\infty} (t - \xi)^2 |A(T, t)|^2 dt \dots\dots\dots (A.5)$$



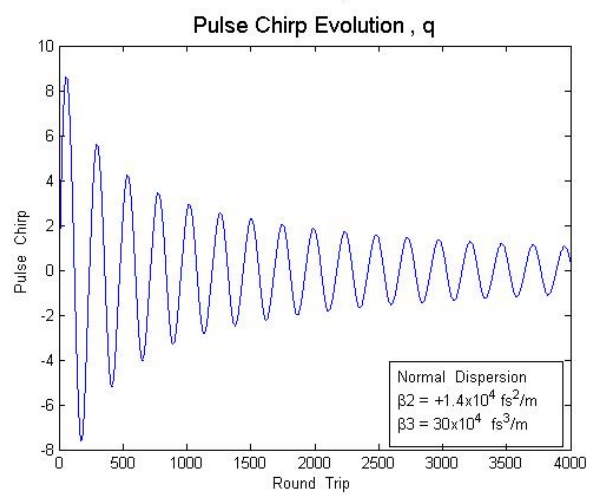
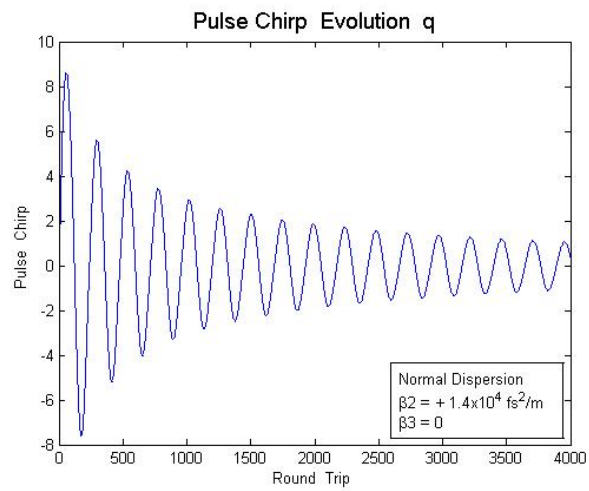


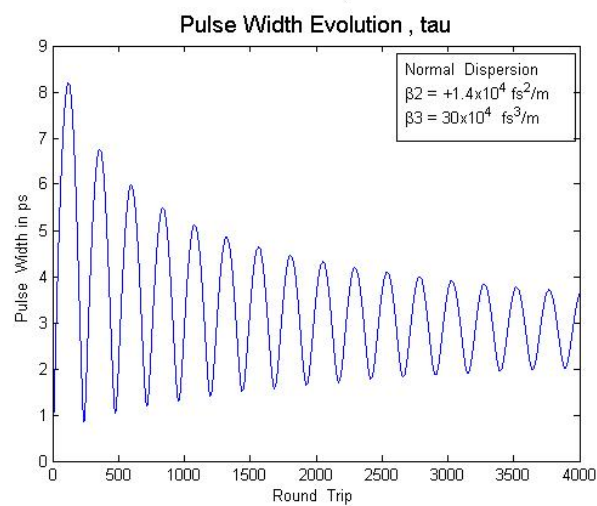
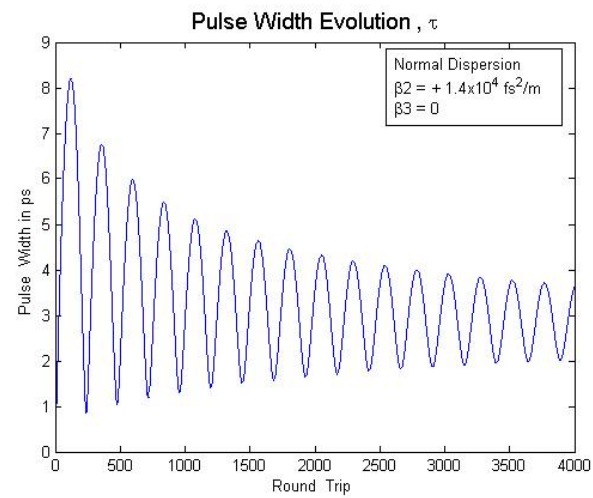


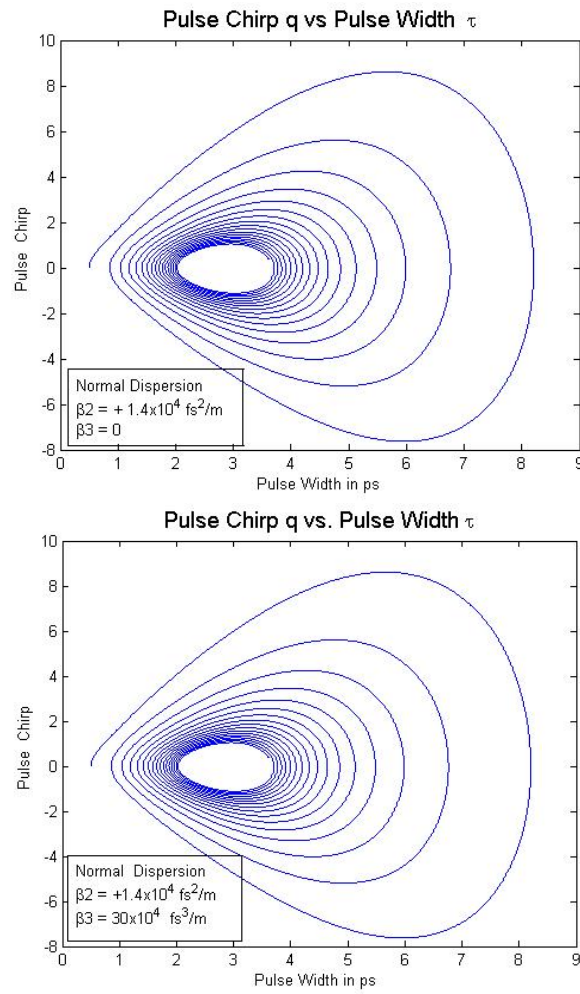
(a)

(b)

Fig. (2): Pulse parameters evolution (Using Table 1): Energy, Temporal and Frequency shift, for Normal regime: (a) Without TOD (b) with TOD





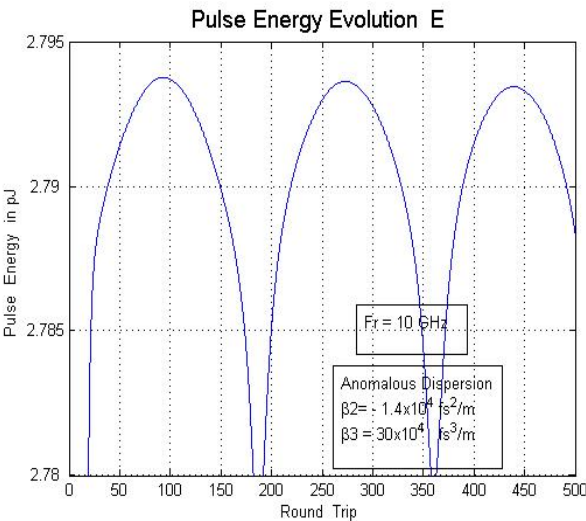
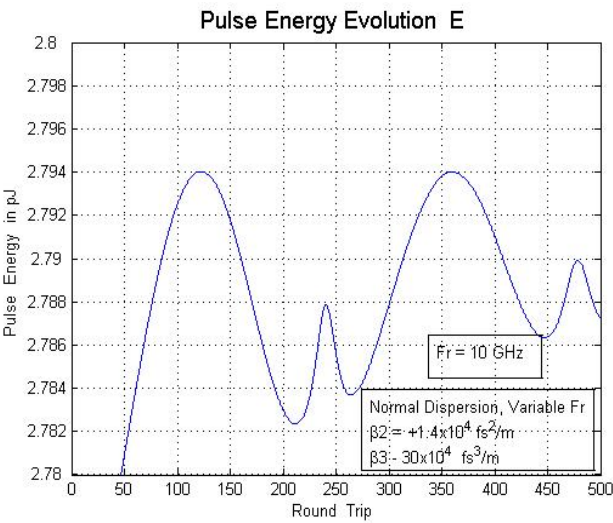


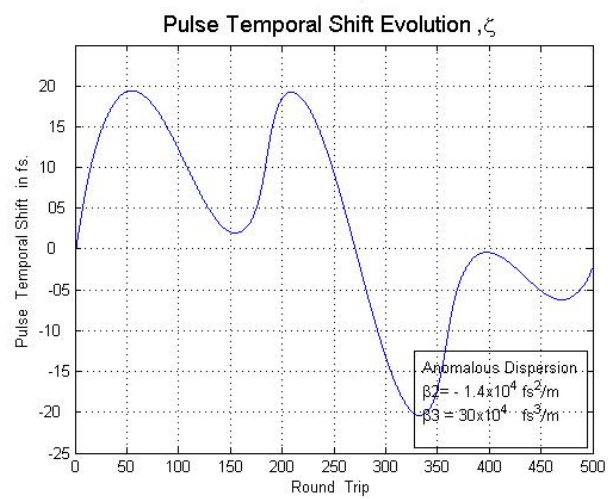
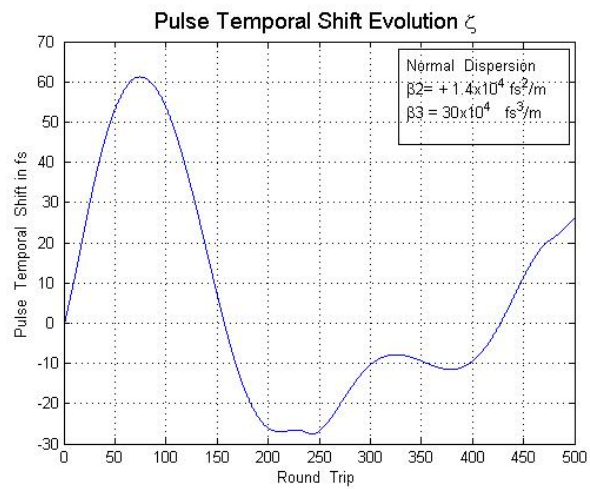
(a)

(b)

Fig. (3): Pulse parameters evolution (Using Table 1): pulse Chirp and Width,
for

Normal regime: (a) without TOD (b) with TOD





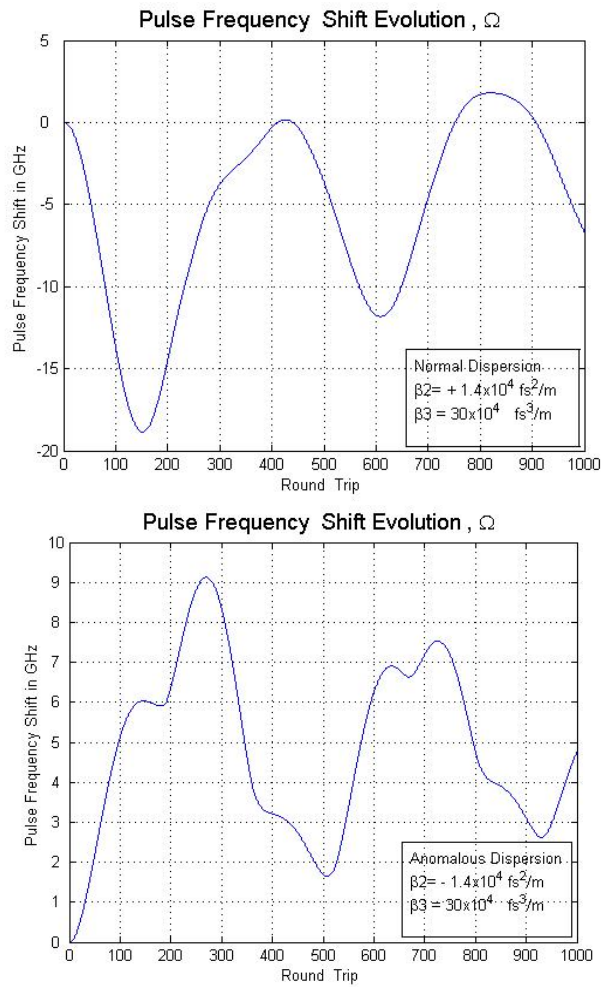
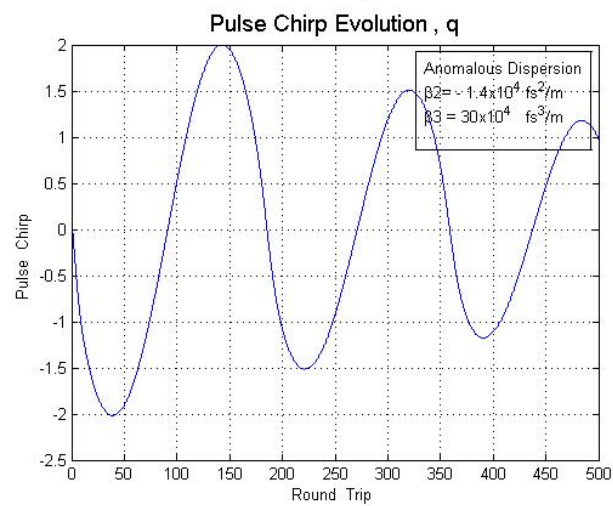
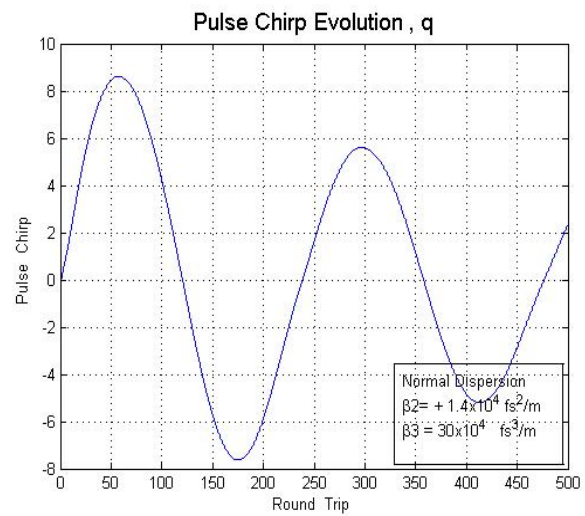


Fig. (4a): Pulse Energy, Temporal and Frequency shift evolution during first roundtrips
(Right) Normal and (Left) Anomalous regime. (Using Table 1)

13



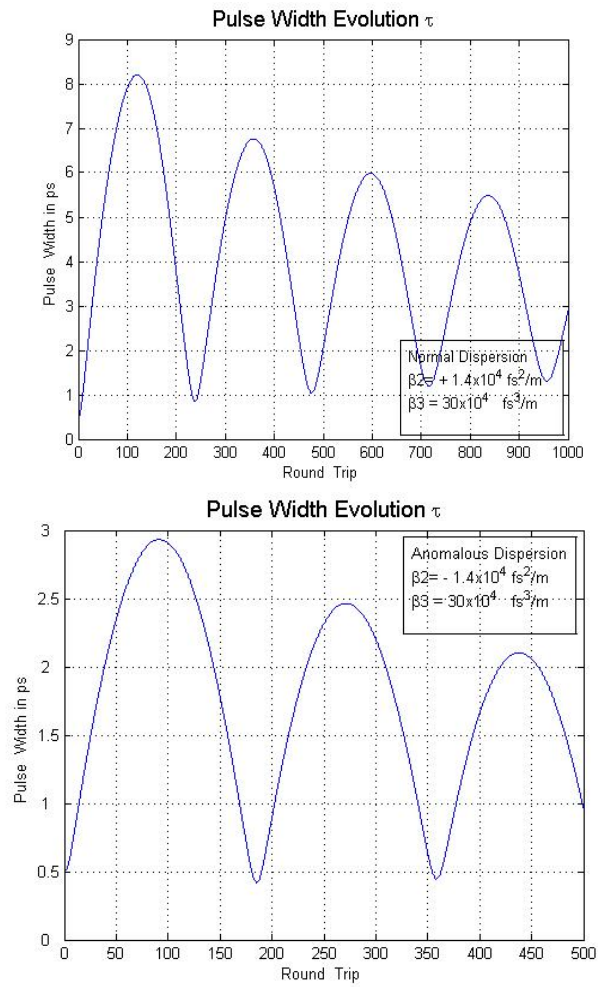
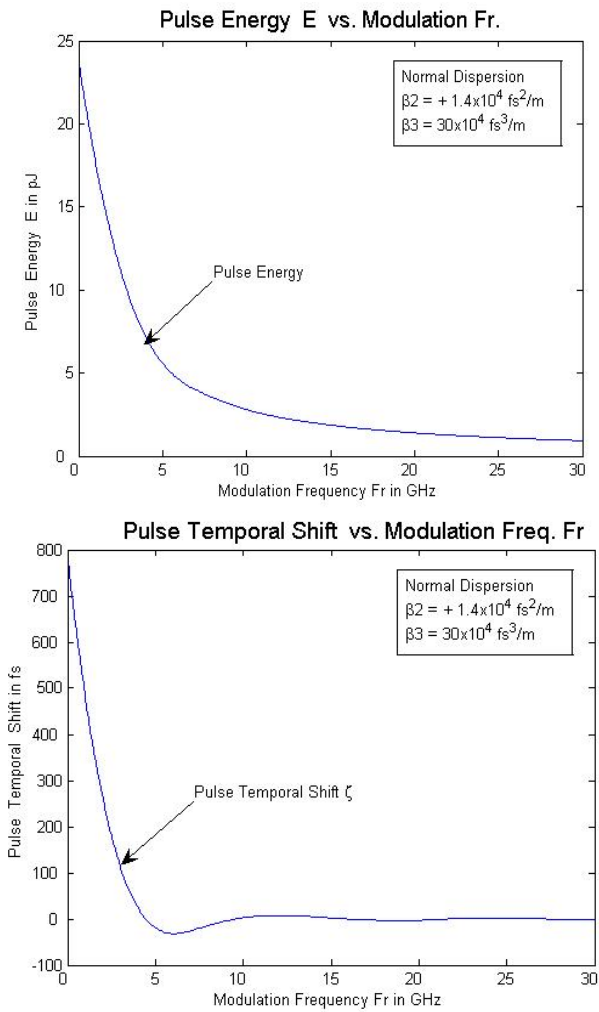


Fig (4b): Pulse Chirp and width evolution during first roundtrips for (Right) Normal and (Left) Anomalous regime . (Using Table 1)



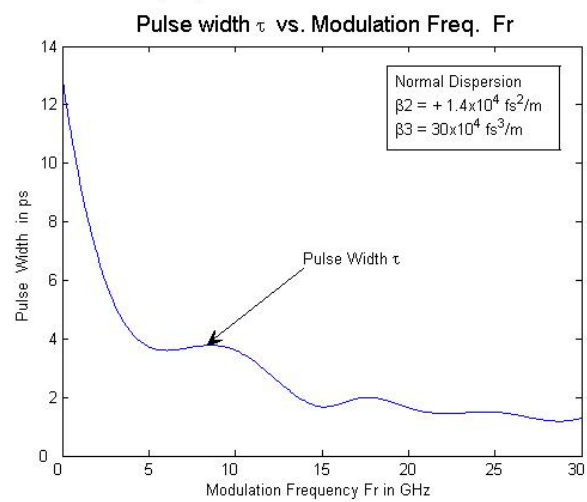
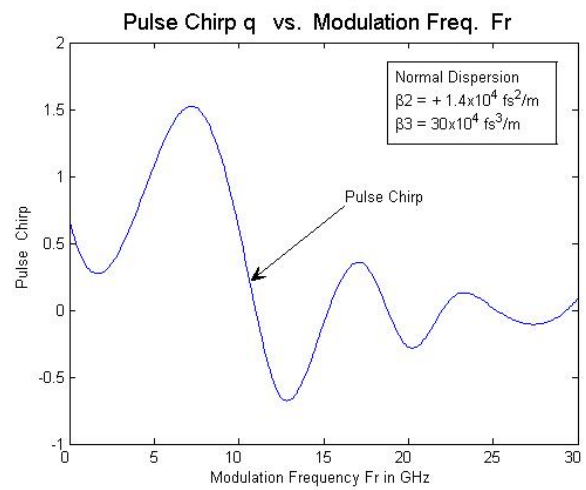
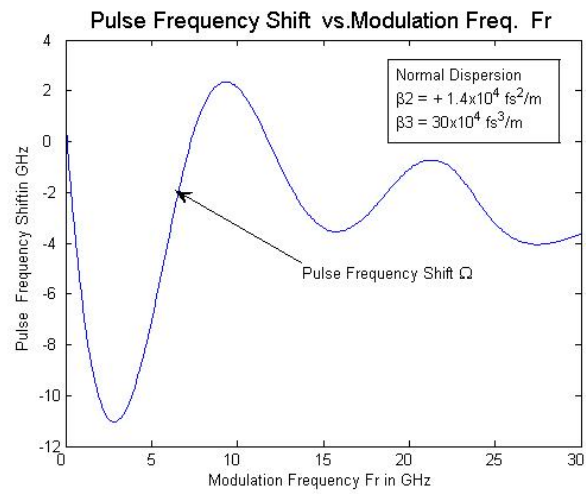
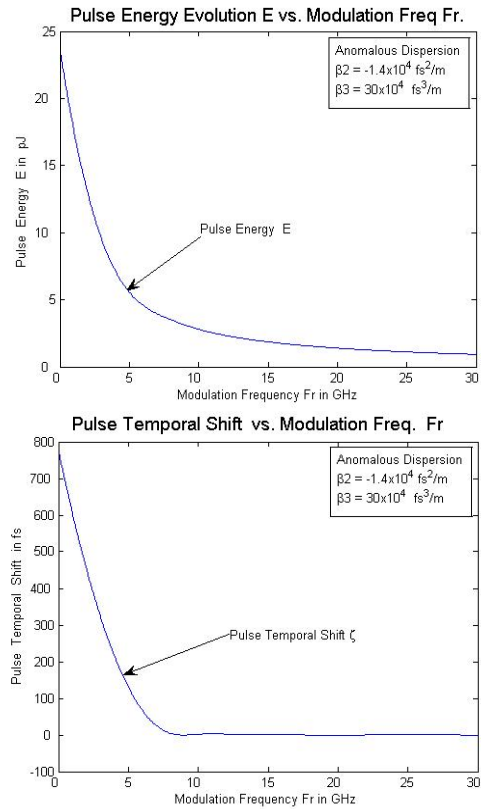


Fig. (5): Pulse Energy, Temporal shift, Frequency shift, Chirp and Width versus modulation frequency in Normal dispersion.

15



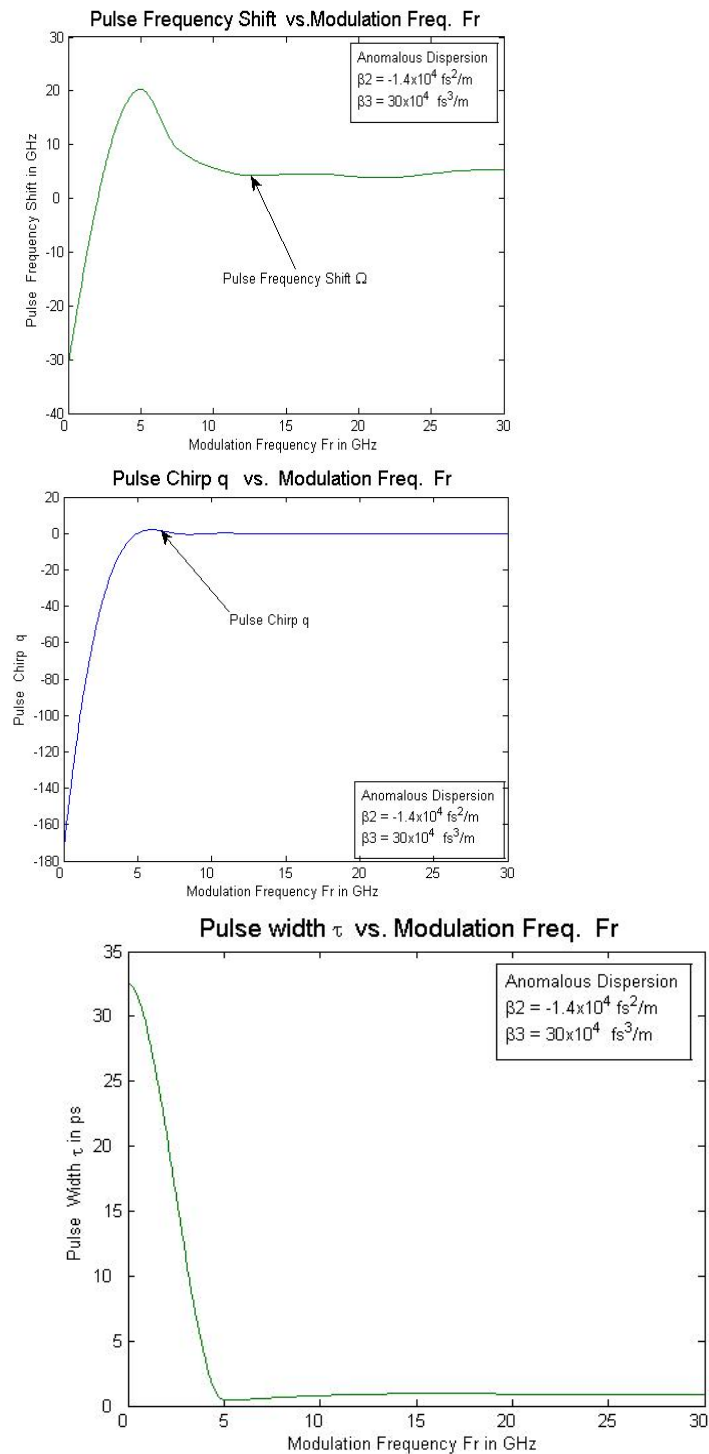


Fig.(6): Pulse Energy, Temporal shift, Frequency shift Chirp and Width versus different modulation frequency in Anomalous dispersion.

